Collective modes of a one-dimensional trapped atomic Bose gas at finite temperatures

Hui Hu[1], Gao Xianlong[2], and Xia-Ji Liu[1],*
[1] *Centre for Quantum and Optical Science, Swinburne University of Technology, Melbourne 3122, Australia and*
[2] *Department of Physics, Zhejiang Normal University, Jinhua 321004, China*
(Dated: February 10, 2014)

We theoretically investigate collective modes of a one-dimensional (1D) interacting Bose gas in harmonic traps at finite temperatures, by using a variational approach and local density approximation. We find that the temperature dependence of collective mode frequencies is notably different in the weakly and strongly interacting regimes. Therefore, the experimental measurement of collective modes could provide a sensitive probe for different quantum phases of a 1D trapped Bose gas, realized by tuning the interatomic interaction strength and temperature. Our prediction on the temperature dependence of the breathing mode frequency is in good qualitative agreement with an earlier experimental measurement for a weakly interacting 1D Bose gas of rubidium-87 atoms in harmonic traps [Moritz *et al.*, Phys. Rev. Lett. **91**, 250402 (2003)].

PACS numbers: 03.75.Kk, 67.85.-d

arXiv:1402.1539v1 [cond-mat.quant-gas] 7 Feb 2014

I. INTRODUCTION

One-dimensional (1D) systems interacting via a delta-function pairwise interparticle interaction are of fundamental importance to many-body physics [1, 2]. Due to the geometric confinement in one dimension, the intrinsic strong correlation between particles may give rise to a number of unusual phenomena, such as effective fermionization, spin-charge separation, prethermalization and non-trivial quench dynamics. The recently realized 1D Bose gas of neutral atoms provides unique opportunities for quantitatively testing and understanding of these unusual phenomena [3–5]. In addition to having the advantage of high degree of control, a 1D atomic Bose gas can be described by the integrable Lieb-Liniger model at arbitrary interaction strengths and finite temperatures [6, 7], which is also exactly solvable with powerful numerical techniques [8] or fundamental mapping theorems [9]. To date, various physical properties of a 1D atomic Bose gas have been investigated both theoretically and experimentally, including the equation of state [10–12], pair correlations [13–16], the momentum distribution [5, 17] and quench dynamics [18].

The purpose of this paper is to provide a systematic theoretical study of collective density oscillations of a 1D trapped Bose gas at finite temperatures. Low-energy collective density modes of a many-particle system are known to give valuable information about its underlying physics, at both zero temperature and finite temperatures. In three dimensions, the measurements of collective density oscillations have verified the superfluid hydrodynamics at the crossover from Bardeen-Cooper-Schrieffer superfluids to Bose-Einstein condensates [19, 20], and have revealed the second sound propagation in strongly interacting unitary Fermi gases [21]. In two dimensions, such measurements may be used to examine the scale invariance satisfied by interatomic interactions [22, 23]. For a 1D Bose gas in harmonic traps with trapping frequency ω_z, collective modes at zero temperature have been extensively investigated and the breathing mode frequency has been shown to increase from $\sqrt{3}\omega_z$ to $2\omega_z$ [3, 24–26], when the cloud crosses from the weakly interacting quasicondensate regime to strongly correlated Tonks-Girardeau (TG) regime. However, surprisingly, less is known about collective modes at finite temperatures, although the first measurement was provided more than ten years ago [3].

In this paper, by using a variational approach [27, 28] together with the exact Yang-Yang equation of state [7], we predict the mode frequency of low-lying collective modes of a 1D trapped Bose gas, at arbitrary interaction strengths and finite temperatures. We show that the temperature dependence of mode frequencies provide a useful means to characterize the different quantum regimes of the 1D Bose cloud. Our exact results allow for a stringent parameter-free comparison with future experimental measurements.

The rest of paper is organized as follows. In the next section, we briefly describe the exact Yang-Yang thermodynamics of a 1D trapped Bose gas within the local density approximation. In Sec. III, we outline the variational approach for the calculation of mode frequencies of low-lying collective modes. In Sec. IV, we first discuss our theoretical results (see, for example, Fig. 3) and then compare the prediction of the breathing mode frequency with the existing experimental measurement (see Fig. 7). Finally, in Sec. V we draw our conclusion.

II. YANG-YANG THERMODYNAMICS OF A 1D TRAPPED BOSE GAS

We consider an atomic gas of N bosons interacting via a pairwise δ-function potential in one dimension in harmonic traps. In the first quantization representation, it can be described by the following Lieb-Liniger Hamilto-

*Electronic address: xiajiliu@swin.edu.au

nian [6],

$$\mathcal{H}_{LL}=\sum_{i}\left[-\frac{\hbar^{2}}{2m}\frac{\partial^{2}}{\partial z_{i}^{2}}+V_{ext}\left(z_{i}\right)\right]+\sum_{i<j}g_{1D}\delta\left(z_{i}-z_{j}\right), \tag{1}$$

where m is the mass of bosons,

$$V_{ext}\left(z\right)=\frac{1}{2}m\omega_{z}^{2}z^{2} \tag{2}$$

is the harmonic trapping potential with frequency ω_z, and g_{1D} (>0) is the only coupling constant used to characterize the short-range repulsive interaction between bosons. In cold-atom laboratory, the 1D configuration can now be routinely realized for atomic gases confined in highly elongated traps or two-dimensional optical lattices, provided that the transverse degrees of freedom are frozen out [3–5].

In the absence of harmonic traps ($V_{ext}=0$), the Lieb-Liniger Hamiltonian is integrable. In 1960s, it was exactly solved by Lieb and Liniger at zero temperature [6] and by Yang and Yang at finite temperatures [7]. By numerically solving two coupled integral equations for the density of quasimomenta and the excitation spectrum [7], all the equations of state, including the number density n, entropy s, energy E and pressure P, can be determined as functions of the chemical potential μ and temperature T, at a given coupling constant g_{1D}. Different quantum phases of the system can be conveniently characterized by using the pair correlation function [13, 14],

$$g^{(2)}\left(z,z\right)=-\frac{1}{n^{2}}\left(\frac{\partial P}{\partial g_{1D}}\right)_{\mu,T}. \tag{3}$$

For an extensive discussion of the Yang-Yang integral equations and finite-temperature pair correlations, we refer to the previous work by Kheruntsyan and his colleagues [14].

With the harmonic trapping potential $V_{ext}(z)\neq 0$, it is convenient to use the local density approximation, which amounts to describing the system locally as a uniform gas with chemical potential equal to the local effective chemical potential,

$$\mu\left(z\right)=\mu-\frac{1}{2}m\omega_{z}^{2}z^{2}, \tag{4}$$

where μ is the global equilibrium chemical potential at the trap center and is determined by the number equation $N=\int_{-\infty}^{+\infty}dzn(z)$. All the thermodynamic variables can then be obtained by integrating the corresponding local quantity over the whole atomic cloud. In particular, the trap-averaged pair correlation is given by,

$$\overline{g^{(2)}}=\frac{\int_{-\infty}^{+\infty}dzg^{(2)}\left(z,z\right)n^{2}\left(z\right)}{\int_{-\infty}^{+\infty}dzn^{2}\left(z\right)}, \tag{5}$$

which can be used to characterize quantum phases in the presence of harmonic traps. We note that the local density approximation is applicable for a large system. For the case of a 1D atomic gas, with typical experimental parameters, a number of atoms $N\sim 100$ is often sufficiently large to ensure the validity of local density approximation [1, 2].

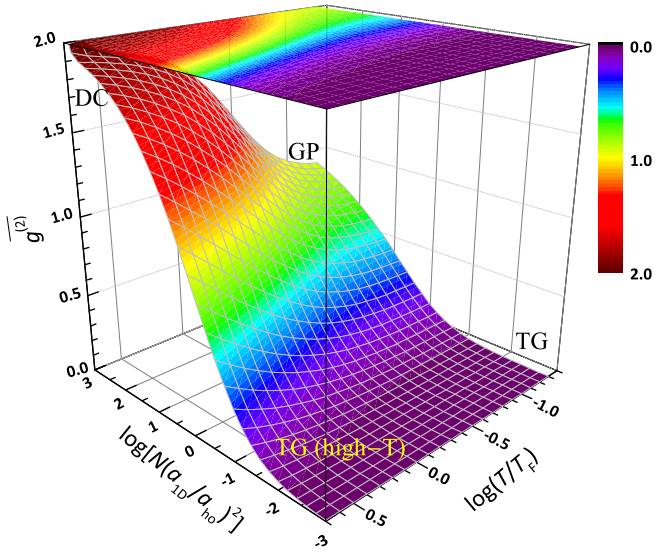

FIG. 1: (Color online) Phase diagram of a trapped 1D interacting Bose gas at finite temperatures. According to the different behavior of the averaged pair correlation function $\overline{g^{(2)}}$, the system can be in the Tonks-Girardeau, Gross-Pitaevskii, or decoherent classical (DC) regime [14]. The transition between different regimes is continuous.

In Fig. 1, we show a contour plot of the averaged pair correlation function $\overline{g^{(2)}}$ as functions of the dimensionless interaction parameter $N(a_{1D}/a_{ho})^2$ and reduced temperature T/T_F, in the logarithmic scale. Here, according to the standard notation for a trapped 1D gas, we have used the 1D scattering length

$$a_{1D}=\frac{2\hbar^{2}}{mg_{1D}} \tag{6}$$

and $a_{ho}=\sqrt{\hbar/(m\omega_z)}$ [29–31]. We have also defined the Fermi temperature $T_F=N\hbar\omega_z$ of an ideal, non-interacting Fermi gas with the same number of atoms as the unit of temperature [29–31]. At low temperatures, in the weakly-interacting Gross-Pitaevskii (GP) and strongly-interacting TG regimes, the trapped Bose gas is characterized by $\overline{g^{(2)}}\simeq 1$ and $\overline{g^{(2)}}\simeq 0$, respectively [13]. With increasing temperature, the weakly interacting Bose cloud quickly turns into a classical Boltzmann gas, which has $\overline{g^{(2)}}\simeq 2$ [14]. In contrast, the pair correlation function of the strongly interacting Bose gas is less affected by temperature, although the system will finally enter a decoherent (quantum) regime at sufficiently high temperatures, in which the pair correlation will also increase to $\overline{g^{(2)}}\simeq 2$ [14].

In Fig. 2, we present the typical density profiles (a, d) and the local pair correlation functions (b, e) in different quantum phases, as a function of the axial coor-

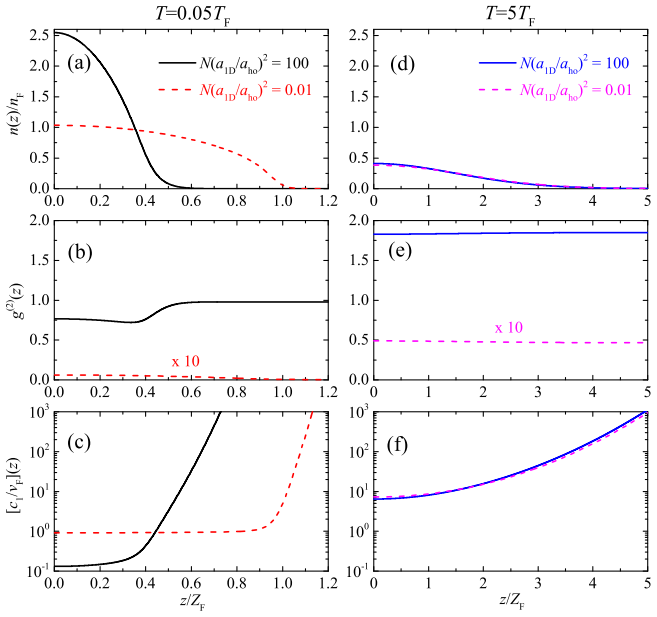

FIG. 2: (Color online) Density profile (a, d), local pair correlation (b, e), and local sound velocity (c, f) in different regimes of temperature and interaction strength. The left and right panels show the results at low ($T = 0.05T_F$) and high temperatures ($T = 5T_F$), respectively. The solid and dashed lines refer to the results at the weak and strong interaction strengths: $N(a_{1D}/a_{ho})^2 = 10^2$ (solid lines) and $N(a_{1D}/a_{ho})^2 = 10^{-2}$ (dashed lines). The density and position are taken in units of the Fermi density and Fermi radius of an ideal, spinless Fermi gas with the same number of atoms, $n_F = \sqrt{2N}/(\pi a_{ho})$ and $Z_F = \sqrt{2N}a_{ho}$, respectively. In the panels (c) and (f), $v_F(z) = \pi\hbar n(z)/m$ is the local Fermi velocity.

dinate normalized to the Fermi radius $Z_F = \sqrt{2N}a_{ho}$. At low temperature ($T = 0.05T_F$), the density profiles and local pair correlation are significantly different in the weak and strong coupling regimes. At high temperature ($T = 5T_F$), while the density profiles of weakly interacting and strongly interacting Bose gases are more or less the same, their local pair correlations differs by about a factor of 40 in magnitude.

III. THEORETICAL FRAMEWORK

At zero temperature, collective density oscillations are governed by the following hydrodynamic equation for the density fluctuation $\delta n(z)$,

$$m\omega^2\delta n\left(z\right)+\frac{\partial}{\partial z}\left\{n\left(z\right)\frac{\partial}{\partial z}\left[\left(\frac{\partial\mu}{\partial n}\right)\delta n\left(z\right)\right]\right\}=0, \quad (7)$$

which has been solved by using sum-rule approach [24] or by deriving analytical or quasi-analytical solutions [25]. At finite temperatures, it is difficult to find a closed equation for the density fluctuation. Instead, collective modes are better described in terms of a displacement field $u(z)$,

$$m\left(\omega^2-\omega_z^2\right)nu\left(z\right)+\frac{\partial}{\partial z}\left[n\left(\frac{\partial P}{\partial n}\right)_{\bar{s}}\frac{\partial u\left(z\right)}{\partial z}\right]=0, \quad (8)$$

where the derivative of the pressure with respect to density is taken at a fixed entropy per particle $\bar{s} = s/n$. The above equation - first derived by Griffin, Wu and Stringari for a collisionally hydrodynamic Bose gas above T_c [32] - can be derived from the standard Landau two-fluid hydrodynamic equations [28]. By using the thermodynamic identity

$$\left(\frac{\partial P}{\partial n}\right)_{\bar{s}}=n\left(\frac{\partial\mu}{\partial n}\right) \quad (9)$$

that is valid at zero temperature and applying the definition of the density fluctuation

$$\delta n\left(z\right)=-\frac{\partial}{\partial z}\left[nu\left(z\right)\right], \quad (10)$$

it is easy to check that at zero temperature Eq. (8) indeed reduces to the equation for density fluctuation Eq. (7).

In the absence of harmonic traps, the solution of Eq. (8) is a plane wave of wave vector q with dispersion $\omega = cq$, where the sound velocity c is given by,

$$c=\sqrt{\frac{1}{m}\left(\frac{\partial P}{\partial n}\right)_{\bar{s}}}. \quad (11)$$

To numerically calculate $(\partial P/\partial n)_{\bar{s}}$, we note that

$$\left(\frac{\partial P}{\partial n}\right)_{\bar{s}}=\frac{\left(P_\mu s_T-P_T s_\mu\right)-\bar{s}\left(P_\mu n_T-P_T n_\mu\right)}{\left(n_\mu s_T-n_T s_\mu\right)}, \quad (12)$$

where we have used the notations such as $P_\mu \equiv (\partial P/\partial\mu)_T$ and $s_T \equiv (\partial s/\partial T)_\mu$. All these first-order derivatives can be obtained numerically by solving the Yang-Yang integral equations [33].

In Figs. 2(c) and 2(f), we report the local sound velocity in units of the local Fermi velocity $v_F(z)$ for different quantum phases of a 1D interacting Bose gas. At low temperatures ($T = 0.05T_F$), sound velocity is dramatically different in the weakly and strongly interacting regimes. However, the difference is washed out quickly by increasing temperature. As a result, far above the degenerate temperature ($T = 5T_F$), sound velocity becomes nearly the same, regardless of the strength of interatomic interactions.

A. Variational approach

In the presence of harmonic traps, the finite-temperature hydrodynamic equation for the displacement field can be solved by using a variational approach [27, 28]. For this purpose, we reformulate it using Hamilton's variational principle and introduce a hydrodynamic

action,

$$S=\int dz\left[m\left(\omega^{2}-\omega_{z}^{2}\right)nu^{2}-n\left(\frac{\partial P}{\partial n}\right)_{\bar{s}}\left(\frac{\partial u}{\partial z}\right)^{2}\right]. \tag{13}$$

All the collective modes can be obtained by minimizing S. Therefore, we consider the following variational (polynomial) ansatz for the displacement field $u\left(z\right)$:

$$u\left(z\right)=\sum_{i=0}^{N_{p}-1}A_{i}z^{i}. \tag{14}$$

The precision of our variational calculations can be improved with increasing N_p, which is the number of the expansion basis $\{A_0, A_1, \cdots, A_{N_p-1}\}$. Inserting the variational displacement field into the action (13), after some straightforward algebra we find that,

$$S=\left[A_{0}^{*},...,A_{i}^{*},...\right]\mathcal{S}\left(\omega\right)\left[A_{0},...,A_{j},...\right]^{T}, \tag{15}$$

where the superscript "T" stands for the transpose of vector and $\mathcal{S}\left(\omega\right)$ is a $N_p \times N_p$ matrix with elements

$$\mathcal{S}_{ij}\left(\omega\right)=\omega^{2}M_{ij}-K_{ij}. \tag{16}$$

Here,

$$M_{ij}=m\int dzn\left(z\right)z^{i+j} \tag{17}$$

and

$$K_{ij}=m\omega_{z}^{2}\int dzn\left(z\right)z^{i+j}+ij\int dzn\left(\frac{\partial P}{\partial n}\right)_{\bar{s}}z^{i+j-2} \tag{18}$$

are the weighted mass moments and the spring constants, respectively. It is readily seen that the minimization of the action S is equivalent to solving

$$\mathcal{S}\left(\omega\right)\left[A_{0},...,A_{j},...\right]^{T}=0 \tag{19}$$

or

$$\det\mathcal{S}\left(\omega\right)=0. \tag{20}$$

B. Dipole mode and breathing mode

It is easy to see that, the dipole mode - for which the displacement field $u(z)$ is a constant - is decoupled from other modes, as a result of the fact that $K_{ij}=\omega_z^2 M_{ij}$ if $i=0$ or $j=0$. This is consistent with Eq. (8), in which the second term involving the equation of state vanishes for a constant displacement field. Hence, the dipole mode is an exact solution of the hydrodynamic equation, with a temperature independent frequency ω_z. In the literature, this is known as Kohn's theorem, which holds for any Galileo transformation invariant systems.

The next mode, the so-called breathing mode, is not an exact solution of the hydrodynamic equation and its mode frequency relies on the equation of state of the system, through the speed of sound $(\partial P/\partial n)_{\bar{s}}$. However, at zero temperature it is known that the displacement $u(z)=A_1 z$ provides an excellent variational ansatz, which essentially becomes exact in the deep weakly interacting GP or strongly interacting TG regimes [24, 25]. As a result, the breathing mode frequency ω_B can be well approximated by,

$$\omega_{B}^{2}\simeq\frac{K_{11}}{M_{11}}=\omega_{z}^{2}+\frac{\int_{-\infty}^{+\infty}dz\left[n\left(\partial P/\partial n\right)_{\bar{s}}\right]}{m\int_{-\infty}^{+\infty}dzn\left(z\right)z^{2}}. \tag{21}$$

Indeed, at zero temperature this sum-rule approach works extremely well [24]. The resulting breathing mode frequency differs very slightly from the exact theory, with a relative error at the order of 0.1% [25].

IV. RESULTS AND DISCUSSIONS

Our variational approach converges very quickly with increasing the number of the variational parameter N_p. The results presented below are calculated with $N_p=8$, for any given temperature T/T_F or dimensionless interaction parameter $N(a_{1D}/a_{ho})^2$.

A. Asymptotic behavior of mode frequencies in some limits

Before discussing our numerical results, it is useful to briefly summarize the known asymptotic behavior of mode frequencies in the low and high temperature limits. At zero temperature, the local chemical potential takes the form $\mu(r)\propto n(r)$ in the weakly interacting GP limit and $\mu(r)\propto n^2(r)$ in the strongly interacting TG limit, respectively. As a result, the hydrodynamic equation at zero temperature Eq. (7) admits exact polynomial solutions with mode frequency [24, 25]

$$\omega_{n}=\sqrt{\frac{n\left(n+1\right)}{2}}\omega_{z} \tag{22}$$

in the GP limit and with frequency [34]

$$\omega_{n}=n\omega_{z} \tag{23}$$

in the TG limit, where the integer $n=1,2,\cdots$ is the index of collective modes. At large temperatures, the equation of state of the Bose gas is well-approximated by the Boltzmann distribution and the density profile takes a gaussian distribution. In this case, the finite temperature hydrodynamic equation Eq. (8) can again admit polynomial solutions. The mode frequency is given by,

$$\omega_{n}=\sqrt{3n-2}\omega_{z}. \tag{24}$$

It is clear that in all cases $\omega_{n=1}=\omega_z$ as required by the Kohn theorem. The breathing mode is the first mode

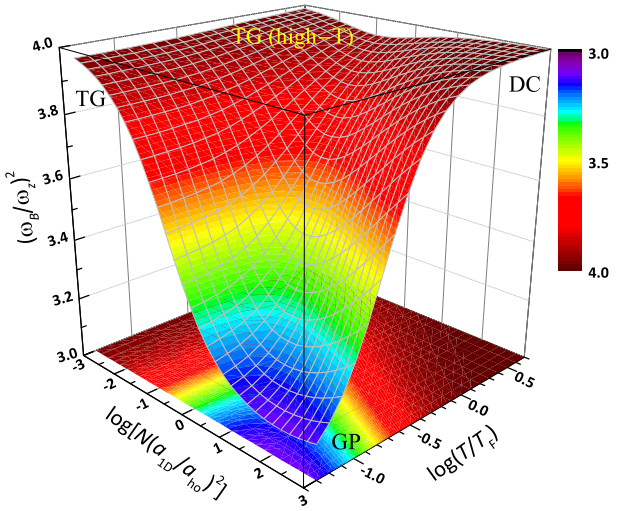

FIG. 3: (Color online) Contour plot of the square of the breathing mode frequency $(\omega_B/\omega_z)^2$ in different regimes. With increasing temperature or interaction strength, the breathing mode frequency increases from $\sqrt{3}\omega_z$ to $2\omega_z$.

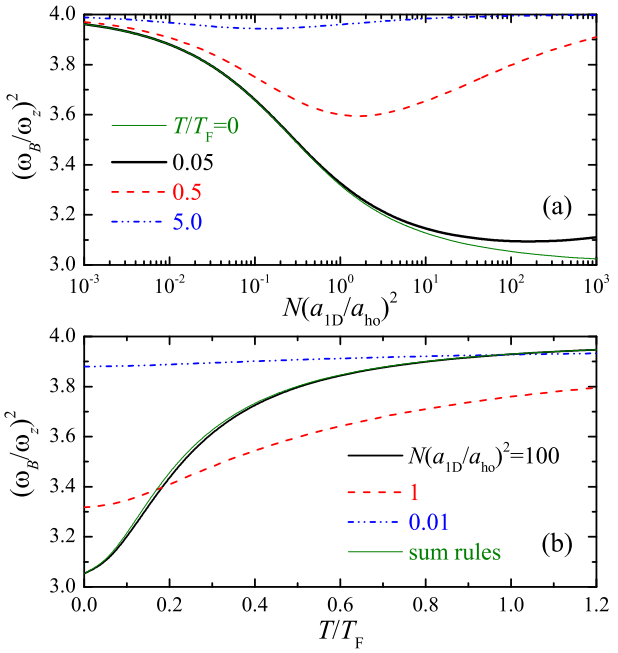

FIG. 4: (Color online) The square of the breathing mode frequency $(\omega_B/\omega_z)^2$ as a function of interaction strength $N(a_{1D}/a_{ho})^2$ (a) or as a function of temperature T/T_F (b). For a weakly interacting Bose gas at $N(a_{1D}/a_{ho})^2 = 100$, the breathing mode frequency obtained by the sum-rules approach is also shown by a thin line in (b).

that has non-trivial temperature dependence. It takes the mode frequency $\omega_B = \sqrt{3}\omega_z$ in the low-temperature mean-field regime and $\omega_B = 2\omega_z$ in either the strongly interacting limit or high-temperature regime.

B. Breathing mode frequency

In Fig. 3, we present a three-dimensional contour plot of the breathing mode frequency. In Figs. 4(a) and 4(b), we plot respectively the coupling constant and temperature dependence of the breathing mode frequency in greater detail. Here, in both figures we show $(\omega_B/\omega_z)^2$ rather than ω_B/ω_z, following the sum-rule convention used in the previous theoretical studies [24].

For the coupling constant dependence, see for example Fig. 4(a), the mode frequency at zero temperature decreases monotonically from the asymptotic strongly interacting value $2\omega_z$ at $N(a_{1D}/a_{ho})^2 \ll 1$ to the weakly interacting value $\sqrt{3}\omega_z$ at $N(a_{1D}/a_{ho})^2 \gg 1$, in agreement with the analytic analysis mentioned earlier. At finite temperatures, however, this monotonic decrease no longer persists. At sufficiently weak coupling, we find that the mode frequency will finally turn up due to a nonzero temperature, whatever how small it is. As a result, a broad minimum appears in the mode frequency, with its position shifting to the strong coupling regime when temperature increases.

For the temperature dependence as shown in Fig. 4(b), we find instead that the mode frequency always increases with increasing temperature at arbitrary interaction strength. In the strongly interacting regime, the trend of increasing becomes very weak, as the zero temperature mode frequency itself shifts to the same value of $2\omega_z$ as in the high temperature limit. We note that, at finite temperatures the sum-rule result Eq. (21) still works excellently well. At the coupling constant $N(a_{1D}/a_{ho})^2 = 100$, the sum-rule result and the full variational prediction for $(\omega_B/\omega_z)^2$ differ in relative by 1% at most, indicating that the breathing mode is indeed well-approximated by the displacement field $u(z) \propto z$.

C. Higher mode frequency

We now consider the mode frequency of higher collective modes. Although these modes are technically more difficult to excite than the breathing mode, their excitations in quasi-1D configuration has been recently demonstrated for a unitary Fermi gas [35]. In Fig. 5, we report the contour plot of the third and fourth compressional modes. The temperature dependence of the frequency of higher modes is presented in Fig. 6.

The qualitative behavior of the frequency of higher collective modes is very similar to what we have observed in the breathing mode. The most remarkable difference is that the mode frequency at zero temperature may significantly be larger than the frequency at high temperatures. As a result, the mode frequency no longer increases monotonically with increasing temperature. Nonetheless, it is clear that all the mode frequencies could have distinct behavior in different quantum phases and hence could provide a useful way to characterize the phase diagram, in addition to the pair correlation characterization.

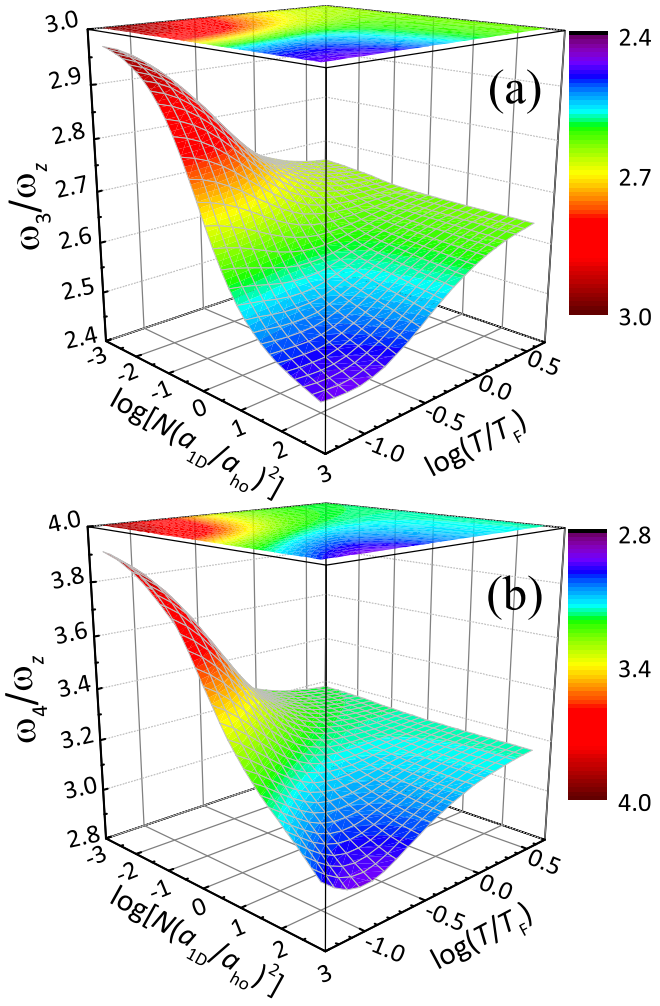

FIG. 5: (Color online) Contour plot of the mode frequency for the third (upper panel, ω_3/ω_z) and fourth (lower panel, ω_4/ω_z) collective modes.

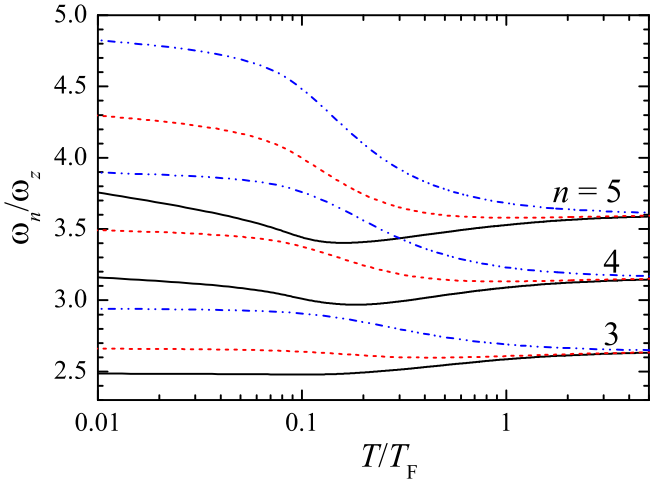

FIG. 6: (Color online) Temperature dependence of the mode frequency for higher-order modes ($n = 3, 4, 5$) at three different interaction strengths: $N(a_{1D}/a_{ho})^2 = 100$ (solid line), 1 (dashed line), and 0.01 (dot-dashed line).

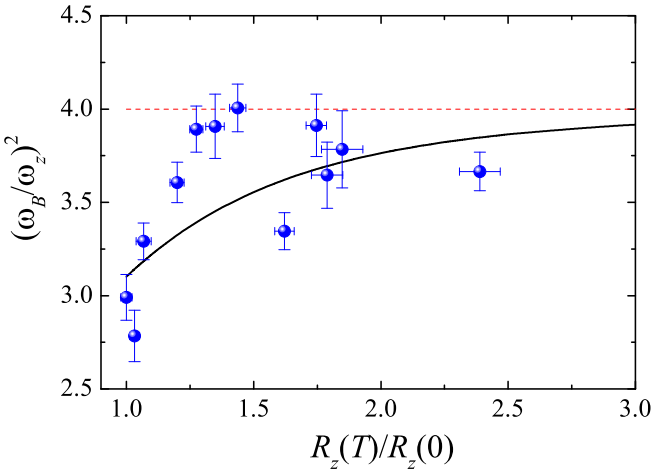

FIG. 7: (Color online) Comparison between our theoretical predictions (solid line) and the experimental data (solid circles with error bars) [3], for the temperature dependence of breathing mode frequency. Experimentally, the temperature is characterized by the rms cloud size $R_z = \sqrt{\langle z^2 \rangle}$ measured after 15 ms of time-of-flight [3]. In the experiment, the coupling constant $N(a_{1D}/a_{ho})^2 \simeq 18$.

D. Comparison with the experiment

Experimentally, the temperature dependence of the breathing mode frequency of a 1D interacting Bose gas at a particular interaction strength was measured by the Esslinger team over ten years ago. The temperature of the atomic cloud is tuned by varying the hold time prior to excitations of the breathing mode and is indirectly characterized by measuring the axial width of the cloud after 15 milliseconds of time-of-flight expansion [3]. Therefore, it is not possible to directly compare our theoretical result of the breathing mode frequency with the experimental data.

In Fig. 7, we compare the theory and experiment by assuming that the normalized cloud size, given by the ratio between the rms axial width at temperature T and at zero temperature $R_z(T)/R_z(0)$, is not affected by the time-of-flight expansion. The agreement between theory and experiment is qualitative good, without any free adjustable parameters. The discrepancy is due to the assumption of invariant ratio $R_z(T)/R_z(0)$ during the time-of-flight expansion as well as the fact that the Bose cloud prior to excitations may not be fully in thermal equilibrium [3]. Refined experimental measurements are required, in order to fully understand the temperature dependence of the breathing mode frequency.

V. CONCLUSIONS

In conclusion, we have investigated the finite-temperature collective modes of a one-dimensional interacting Bose gas in harmonic traps, which are described

by the Landau hydrodynamic equation. We have used Hamilton's variational principle and have derived a variational action for solving the hydrodynamic equation. By taking a polynomial variational ansatz, we have accurately calculated the frequency of collective modes at arbitrary temperature and interaction strength.

The mode frequency of collective modes, particularly the breathing mode frequency, is found to have pronounced temperature dependence in different quantum phases in the weak and strong coupling regimes. As a result, experimental measurement of collective modes could provide a sensitive probe of the phase diagram of a one-dimensional trapped Bose gas, complementing the proposed characterization of pair-correlation functions at finite temperatures [13, 14]. We have shown that our theoretical prediction on the temperature dependence of the breathing mode frequency is in good qualitative agreement with an earlier experimental measurement for a weakly interacting 1D Bose gas of rubidium-87 atoms in harmonic traps [3]. Quantitative test of our theory could be obtained in the near future with high-precision measurements for collective modes.

Acknowledgments

HH and XJL were supported by the ARC Discovery Projects (Grant Nos. FT130100815, DP140103231 and DP140100637) and NFRP-China (Grant No. 2011CB921502). GX was supported by the Zhejiang Provincial Natural Science Foundation under Grant No. R6110175.

Note added. — In completing our numerical calculations, we become aware of a recent experimental measurement of the breathing mode in 1D atomic Bose gases reported by Isabelle Bouchoule and co-workers [36]. In their preprint, the breathing mode frequency has also been theoretically calculated by directly solving the coupled hydrodynamic equation for small density fluctuations.

[1] M. A. Cazalilla, R. Citro, T. Giamarchi, E. Orignac, and M. Rigol, Rev. Mod. Phys. **83**, 1405 (2011).

[2] X.-W. Guan, M. T. Batchelor, and C. Lee, Rev. Mod. Phys. **85**, 1633 (2013).

[3] H. Moritz, T. Stöferle, M. Köhl, and T. Esslinger, Phys. Rev. Lett. **91**, 250402 (2003).

[4] T. Kinoshita, T. Wenger, and D. Weiss, Science **305**, 1125 (2004).

[5] B. Paredes, A.Widera, V. Murg, O. Mandel, S. Fölling, I. Cirac, G. Shlyapnikov, T. Hänsch, and I. Bloch, Nature (London) **429**, 277 (2004).

[6] E. H. Lieb and W. Liniger, Phys. Rev. **130**, 1605 (1963); E. H. Lieb, Phys. Rev. **130**, 1616 (1963).

[7] C. N. Yang and C. P. Yang, J. Math. Phys. **10**, 1115 (1969).

[8] U. Schollwöck, Rev. Mod. Phys. **77**, 259 (2005).

[9] M. Girardeau, J. Math. Phys. (N.Y.) **1**, 516 (1960).

[10] A. H. van Amerongen, J. J. P. van Es, P. Wicke, K. V. Kheruntsyan, and N. J. van Druten, Phys. Rev. Lett. **100**, 090402 (2008).

[11] T. Jacqmin, J. Armijo, T. Berrada, K. V. Kheruntsyan, and I. Bouchoule, Phys. Rev. Lett. **106**, 230405 (2011).

[12] A. Vogler, R. Labouvie, F. Stubenrauch, G. Barontini, V. Guarrera, and H. Ott, Phys. Rev. A **88**, 031603(R) (2013).

[13] K. V. Kheruntsyan, D. M. Gangardt, P. D. Drummond, and G. V. Shlyapnikov, Phys. Rev. Lett. **91**, 040403 (2003).

[14] K. V. Kheruntsyan, D. M. Gangardt, P. D. Drummond, and G. V. Shlyapnikov, Phys. Rev. A **71**, 053615 (2005).

[15] T. Kinoshita, T. Wenger, and D. S. Weiss, Phys. Rev. Lett. **95**, 190406 (2005).

[16] J. Esteve, J.-B. Trebbia, T. Schumm, A. Aspect, C. I.Westbrook, and I. Bouchoule, Phys. Rev. Lett. **96**, 130403 (2006).

[17] M. J. Davis, P. B. Blakie, A.H. van Amerongen, N. J. vanDruten, and K. V. Kheruntsyan, Phys. Rev. A **85**, 031604 (2012).

[18] M. Cheneau, P. Barmettler, D. Poletti, M. Endres, P. Schauß, T. Fukuhara, C. Gross, I. Bloch, C. Kollath, and S. Kuhr, Nature (London) **481**, 484 (2012).

[19] H. Hu, A. Minguzzi, X.-J. Liu, and M. P. Tosi, Phys. Rev. Lett. **93**, 190403 (2004).

[20] A. Altmeyer, S. Riedl, C. Kohstall, M. J. Wright, R. Geursen, M. Bartenstein, C. Chin, J. Hecker Denschlag, and R. Grimm, Phys. Rev. Lett. **98** 040401 (2007).

[21] L. A. Sidorenkov, M. K. Tey, R. Grimm, Y.-H. Hou, L. Pitaevskii, and S. Stringari, Nature (London) **498**, 78 (2013).

[22] L. P. Pitaevskii and A. Rosch, Phys. Rev. A **55**, R853 (1997).

[23] E. Vogt, M. Feld, B. Fröhlich, D. Pertot, M. Koschorreck, and M. Köhl, Phys. Rev. Lett. **108**, 070404 (2012).

[24] C. Menotti and S. Stringari, Phys. Rev. A **66**, 043610 (2002).

[25] J. N. Fuchs, X. Leyronas, and R. Combescot Phys. Rev. A **68**, 043610 (2003).

[26] E. Haller, M. Gustavsson, M. Mark, J. Danzl, R. Hart, G. Pupillo, and H. Nägerl, Science **325**, 1224 (2009).

[27] E. Taylor, H. Hu, X.-J. Liu, and A. Griffin, Phys. Rev. A **77**, 033608 (2008).

[28] E. Taylor, H. Hu, X.-J. Liu, L. P. Pitaevskii, A. Griffin, and S. Stringari, Phys. Rev. A **80**, 053601 (2009).

[29] H. Hu, X.-J. Liu, and P. D. Drummond, Phys. Rev. Lett. **98**, 070403 (2007).

[30] X.-J. Liu, H. Hu, and P. D. Drummond, Phys. Rev. A **76**, 043605 (2007).

[31] X.-J. Liu, H. Hu, and P. D. Drummond, Phys. Rev. A **78**, 023601 (2008).

[32] A. Griffin, W.-C. Wu, and S. Stringari, Phys. Rev. Lett. **78**, 1838 (1997).

[33] As an important check for numerical accuracy, we use the

thermodynamic relations, $P_\mu = n$, $P_T = s$, and $s_\mu = n_T$.
[34] A. Minguzzi, P. Vignolo, M. L. Chiofalo, and M. P. Tosi, Phys. Rev. A **64**, 033605 (2001).
[35] M. K. Tey, L. A. Sidorenkov, E. R. Sánchez Guajardo, R. Grimm, M. J. H. Ku, M. W. Zwierlein, Y. H. Hou, L. Pitaevskii, and S. Stringari, Phys. Rev. Lett. **110**, 055303 (2013).
[36] B. Fang, G. Carleo, and I. Bouchoule, arXiv:1312.3169 (2013).